DOI: 10.13009/EUCASS2022-7674
9TH EUROPEAN CONFERENCE FOR AERONAUTICS AND SPACE SCIENCES (EUCASS)

PERSEUS and Innovative Propulsion Laboratory Project Design of a motopump lox

Emrys BOUISSON, Pascal PEMPIE** et al.*
** Innovative Propulsion Laboratory, 94200, Ivry-sur-Seine, France*
emrys.bouisson@ipsa.fr
***PERSEUS, Coordinator, CNES, pascal.pempie@wanadoo.fr*

Abstract
In a context of innovation, the PERSEUS program aims to set up ground and flight demonstrator projects by students. This is why, in order to improve the MINERVA engine, we were asked to design an oxygen motor pump. We will see how the design of the various parts were made but also the choice of certain elements like the joints, the bearings or also the motorization. As well as numerical simulations to have a verification of the design and an overture on the tests to come.

Nomenclature

P_0	Inlet Pressure
P_2	Outlet Pressure
ΔP	Difference Pressure
ΔH	Difference dynamic head
Ht	Total dynamic head
ΔP_u	Difference useful pressure
T	Temperature of oxygen
$NPSP$	Net positive suction pressure
$NPSH$	Net positive suction head
$\dot{m}$	Mass flow
D_v	Volumetric flow
ρ	Density of oxygen
W_u	Useful power
W_t	Total power
Ns	Specific speed
N	Rotation speed
S	Specific speed aspiration
μ	Trace constant
Ds	Specific diameter
ν	Efficiency
ν_h	Volumetric efficiency
Z	Number of blade
β_2	Outlet angle of blade
σ	Slip factor
U_0	Inlet peripheric speed of the impeller
V_0	Inlet absolute speed of the impeller
W_0	Inlet relative speed of the impeller
U_2	Outlet speed of the impeller
V_{m2}	Meridional outlet speed of the impeller
V_{u2}	Useful outlet absolute speed of the impeller

DOI: 10.13009/EUCASS2022-7674

V_2	Outlet absolute speed of the impeller
W_2	Outlet relative speed of the impeller
D_0	Inlet diameter of the impeller
D_2	Outlet diameter of the impeller
b_2	Outlet Height of the impeller
F_a	Removed force from the ribs
d_r	Diameter of the ribs
d_s	Diameter of the shaft
g	Gravitational force
s	Height between the wheel and the volute
t	Height of the ribs
Q_b	Cooling flow
F_b	Bearing force
C_p	Heat capacity of oxygen

1. Introduction

The easiest way to make a liquid propellant engine for a suborbital rocket is to use a pressure fed engine. These engines are powered by propellants put under pressure in tanks. These classes of engines do not require turbomachines, which simplifies the design and allows for better reliability. This is why the first PERSEUS liquid propellant rocket will be powered by a pressure fed engine, MINERVA. This engine will use the LOX/Ethanol propellants and will have 5 kN of thrust.
However, due to the fact that the propellants are under pressure in the tanks, these pressures cannot be very high. The higher the pressure, the thicker the tanks will need to be, which implies that the on-board weight will be increased. We are thus obliged to limit the pressure in order not to increase the tank's dry mass. The chamber pressure being limited, the performance of the engine will also be limited. This is why the pressure fed version of the MINERVA will not be able to exceed 5 kN.
To increase the engine's performance, it is therefore necessary to increase the propellant pressure at the combustion chamber inlet. And for that, it is necessary to use pumps. They can be powered by a turbine or by an electric motor. For reasons of complexity, we will use electric motors. The goal of these motopumps is to increase the thrust of the MINERVA engine from 5 kN to 10 kN.

2. Objectives

The goal is to design a pump powered by an electric motor. That will make it possible to supply with propellants an engine which will have a thrust of 10 kN. The pump shall have the following characteristics:

Table 1: Characteristics of the pump

	Fluid	**T (K)**	**P_0 (bar)**	**P_2 (bar)**	**$\dot{m}$ (kg/s)**	**Security coefficient**	**breaking limit**	**pressure loss coefficient**
Data	Lox	90	3	52	2.45	1.15	1.25	1.3

The design of the motopump takes into consideration the following elements:

- Design of the wheel
- Design of the volute
- Materials
- Choice of seals and bearings
- Choice of motorisation

DOI: 10.13009/EUCASS2022-7674

3. Conception

3.1 Pre-sizing

Pump pre-sizing is an important and necessary part of pump design. It allows to determine global parameters such as the number of rotations per minute, the diameter, output speed, required power and many others.
For pre-sizing, it is necessary to know the specifications that the pump must have. The specifications for this motopump are as follows:

Table 2: Specifications of the pump

	P_0 (bar)	T (K)	P_2 (bar)	NPSP (bar)	$\dot{m}$ (kg/s)	Fluid	ρ (kg/m^3)
Data	3	90	52	0.9442	2.45	Lox	1140

Using the formulas in [1] and [2], we can obtain the following initial data:

Table 3: Initial data of the pump

	ΔP (bar)	ΔH (m)	ΔH (ft)	D_v (m^3/s)	D_v (gpm)	NPSH (m)	W_u (kw)
Data	49	438.149	1 437.568	0.00215	34.064	8.554	10.531

To continue the pre-sizing, we sought to get closer to a specific yield. The chosen yield is $\nu = 0.75$. This is a quite good performance, included in the average of pump, and it is not necessary to have a higher yield because it would be complex to achieve in real conditions.
To estimate the yield, we use the following graph:

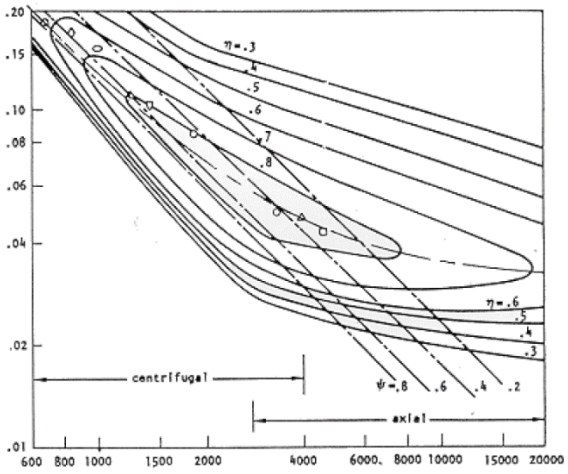

Figure 1: Efficiency according to of Ds as a function of Ns

Following the calculation steps in [1] and [2] and tables 2 and 3, after a number of iterations, we were able to obtain the following values with an efficiency $\nu = 0.718$:

Table 4: Pre-sizing of the pump

	Ns	Ns (US)	N (rpm)	S	μ	U_2 (m/s)	D_2 (mm)	D_2 (ft)	Ds	Ds (US)	ν	W_t (kW)
Data	22.0	1 136.37	45 450	421.234	0.422	100.93	42.42	0.139	4.186	0.148	0.718	14.67

We validated this yield, which is different from the one targeted, because we did not find a configuration with a better yield.

DOI: 10.13009/EUCASS2022-7674

3.2 General sizing

All the calculations in this section, except for the ones specifically mentioned, are presented in [1] and [2].

The first step is to size the pump impeller. After some iterations, we decided to take $d_1 = 16\,mm$. The following values were then obtained:

Table 5: Inlet data of the impeller

	D_0 (mm)	U_0 (m/s)	V_0 (m/s)	W_0 (m/s)	NPSH ($\lambda = 0.2$)	NPSH ($\lambda = 0.15$)
Data	1.80×10^{-2}	42.84	40.82	59.17	120.60	111.68

From these results, we can see that the pump will need an inducer in order to function because otherwise, due to strong suction, cavitation can form and create important damage to the pump.
Then we can determine the inlet angles of the impeller blades. We have $\beta_1(fluid) = 6.203\,°$ and $\beta_2 = 10.203\,°$. We also have the minimum suction pressure of the impeller which is $P_1 = 7.219$ bar.

Using that input data, we can work out the following output data:

Table 6: Outlet data of the impeller

	U_2 (m/s)	V_{m2} (m/s)	b_2 (mm)	ν_h	Ht (m)	Z
Data	100.93	100.93	1.88	0.772	567.55	7

We notice that b_2 is small. To limit some constraints related to this, we decided to have only a lower flange and to remove the upper flange. This will slightly decrease the efficiency but will make the design and manufacturing easier. With this information, we are able to determine the exit angle of the impeller as well as the exit speeds:

Table 7: Outlet angle of the impeller

	β_2 (°)	σ	V_{u2} (m/s)	Ht (m)	β_2(fluid)(°)	V_2 (m/s)	W_2 (m/s)
Data	15	0.869	55.02	566.07	12.40	55.94	47.01

Following this information, we can determine the static pressure present in the wheel. We obtain the following values:

Table 8: Pressure in the impeller

	ΔP (bar)	ν_h	ΔP_u (bar)	P_2 (bar)
Data	45.13	0.772	34.84	42.06

In the end, we can calculate the total pressure generated by the wheel. We have $P_{02} = 55.45$ bar.

DOI: 10.13009/EUCASS2022-7674

3.3 Modelling

With the tables 2 to 8, as well as the CFTurbo software we can obtain a global model of the pump. The software allowed us to correctly determine the shape of the impeller and the inducer blades so that the pump can provide the desired pressures.
According to the software we obtain the following pressure profiles:

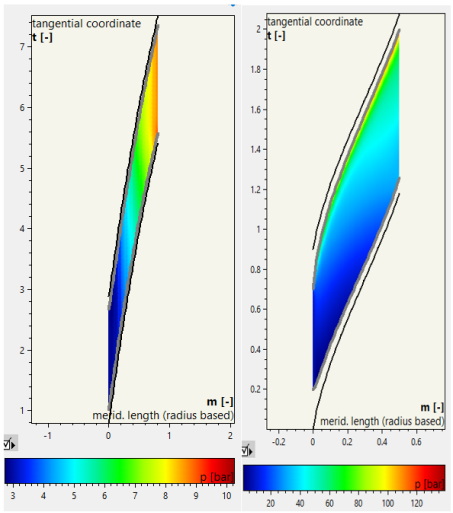

Figure 2: Pressure profiles of inducer (left) and impeller (right)

We can see that the pressures are consistent with the different values from the previous tables. With a pressure at the inducer outlet and impeller inlet higher than 7.219 bar, as well as an average pressure at the impeller outlet close to 55 bar. Moreover, we can notice that there is no pressure drop at the inducer, which shows that there is no major risk of damage due to cavitation. CFD simulations will be necessary when the pump will be designed to validate its proper operation.
After validation of the profiles of the blades as well as their numbers, we were able to extract them to model the pump on the modelling software CATIA.
Some modifications had to be done for manufacturing constraints. Indeed, the shape of the blades is complex, and the pump is small. It was thus necessary to adapt slightly certain parts of the pump so that it can be manufactured.

The pump model had to be enriched with new elements to be able to take into account the forces that the pump generates during its operation.
In a pump, there are different types of forces that can cause instabilities and damage the pump. First of all, the radial forces:
The impeller of a centrifugal pump moves the fluid out radially. However, because the impeller is a spiral, the resulting forces of the pressures will not be equal and there will be an imbalance.
There are two main solutions to this. The first one is the installation of a double volute in order to have a symmetry of the spiral and thus to have symmetrical forces. And the second one is the installation of a fixed diffuser which will allow equalization of the forces. Because of the size of our pump, we have opted to use a double volute for ease of design and manufacturing.

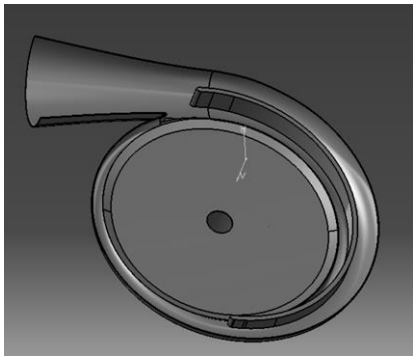

DOI: 10.13009/EUCASS2022-7674

Figure 3: Double Volute of the pump

In addition, the pump also generates axial forces, due to the pressure difference between the top and bottom of the impeller. These forces will create vertical movements along the axis of rotation and can damage all parts in contact with the drive shaft.
To overcome this problem, there are various methods. The first is to use ribs under the impeller, they will reduce the pressure under the impeller and thus reduce the forces. The second is to make a balancing chamber under the impeller, again to reduce the pressure by putting fluid at the same pressure as the inlet. The third is the use of a balancing piston, the goal being to submit to the same pressure constraints as the impeller on a piston but inverted to have a resultant of zero forces.
Following the calculation of axial forces in [1], we find that the resultant of the forces is $F = -4440$ N.
With the resultant we find, we can conclude that we need to balance the wheel. However, as the force is not so high, we decided to use the method of the ribs on the back of the wheel. The following formula, allows us to know the cancelled forces according to their dimensions (caution, formula in imperial system):

$$F_a = \frac{\frac{3\pi}{4\,608}(d_r^2 - d_s^2)}{2g}\rho\frac{(s+t)}{2s} \tag{1}$$

Using this formula, we were able to determine a rib size to reduce the axial forces by half, which is now around 2300 N. This force is low enough that the bearings, dynamic seals and coupler can withstand it. The blades have the following dimensions:

Table 9: Size of the ribs

	Length (mm)	**Width (mm)**	**Height (mm)**
Data	13.5	0.8	1

In the end we obtain the following wheel and volute:

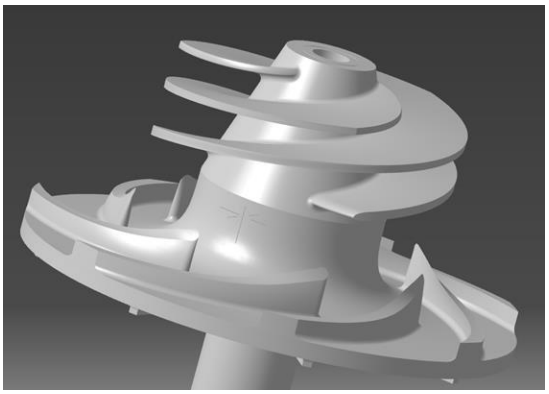

Figure 4: Wheel of the pump

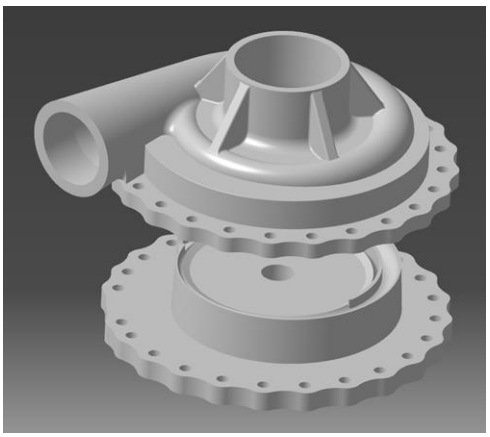

Figure 5: Volute of the wheel

DOI: 10.13009/EUCASS2022-7674

3.4 Materials

For a motopump where a cryogenic fluid, such as liquid oxygen, circulates, the choice of materials to use is important. In addition to undergoing significant stresses due to the pressures involved, there are oxidation stresses due to the oxygen and thermal stresses in relation to the temperature because during operation, the nominal temperature is 90 K (-183 °C).
The materials we have to choose must have a very good mechanical resistance at ambient temperature (for tests with water) as well as at cryogenic temperatures, be able to resist an extremely oxidizing environment and be able to be used in cryogenic conditions.
After analysing different materials, we were able to find two metals that could satisfy our needs. They are 310 stainless steel and Inconel 718.
For the impeller, we initially chose Inconel 718, however the impeller is machined, and this metal is very complicated to machine because of its very high strength, so we decided that the impeller will be made of stainless steel 310 which has a very good mechanical strength with a yield strength of 310 MPa at room temperature and 585 MPa at cryogenic temperatures.
For the volute, we do not know yet what material it will be made of. We do not know yet if we will use 3D printing or machining to make it. If we choose the 3D printing, the Inconel 718 could be used and if we choose the machining the stainless steel 310 will be considered.

3.5 Bearings/Seals

The bearings are going to make the connection between the rotating part and the fixed part of the pump. In our case, the bearings will undergo certain constraints which require particular characteristics.
Indeed, the bearings will undergo an axial stress which is not negligible, about 2 300 N. Then they must resist a high rotation speed, 45 450 rpm. And they must be able to operate in a very oxidizing environment with cryogenic temperatures. It is expected to have two bearings for the pump.
The characteristics that a bearing supplier gave us are as follow:

Table 10: Characteristics of the bearing

	Materials	**Ball**	**Preload**	**Lubrication**	**Feature**
Data	Rings: cronidur 30 Balls: ceramic Cage: PTFE	Diameter: 4.763 mm Number 10	500 N back to back	Dry: MoS_4	Treated for cryogenic application

During the operation of the pump, the bearings' temperature will increase and if it increases too much, the bearings will break. That's why the bearings must have a cooling system.
In this case, we cannot use oil to cool the bearings because of the cryogenic temperatures. So, we will use liquid oxygen that passes through the pump to cool the bearings.
We are going to make a circuit which will recover the oxygen at the exit of the pump, to then bring it towards the bearings before making it return at the entry of the pump to minimize losses.
The following formula allows us to know the volumetric flow rate necessary to cool the bearings:

$$Q_b = \frac{F_b}{C_p \times \rho \times \Delta T} \tag{2}$$

Now we can know the flow rate needed to cool the bearings. This flow is $Q_b = 1.53 \times 10^{-5}\ \ m^3/s$. This corresponds to 0.71% of the total pump flow, which represents a sufficiently small loss.

The seals will ensure both the sealing between the different fixed parts and the sealing between the rotating part and the fixed parts. It is therefore necessary to have static and dynamic seals. These seals will have to resist to different types of constraints which are to be able to operate in an oxidizing environment and with cryogenic temperatures.

The pump will need to have static seals at different locations. They are the inlet and outlet of the pump as well as between the two parts of the volute and at the casing containing the dynamic seals and bearings. These seals will not be subject to much pressure stress.
For these seals, PTFE O-rings are sufficient given the different stresses.

DOI: 10.13009/EUCASS2022-7674

The pump should have several dynamic seals. The first location is between the bottom of the impeller and the first bearing, and the second location is after the second bearing. Unlike static seals, the stresses of dynamic seals are much higher. Indeed, we have quite high speeds, about 20 m/s, in addition to cryogenic temperatures and a small size. All these constraints make finding a dynamic joint that respects all the nominal conditions difficult.
We were able to find dynamic joints that fit our constraints. These joints are made of UHMW and stainless steel. They resist up to 40 MPa and cryogenic temperatures. However, their maximum speed is 15 m/s and our speed is 20 m/s, so these joints are limited. However, since the duration of use is short it is possible to use them.

3.6 Motorisation

The motor pump that we want to create must be driven by an electric motor. Following this need, it was defined an operating point for the motor: a power of approximately 14 kW and a rotational speed of approximately 45 500 rpm. "Brushless" motors are preferred to limit as much as possible the risks related to the liquid oxygen. We are also looking to obtain these performances under a power supply well below 100 V. Finally, the weight and the price must not be excessive.
A German company (Lehner Motoren Technik) offers motors providing the required performances, especially in terms of rotation speed.
Moreover, the proposed products are mass-produced and not custom-made, drastically reducing the price of the motor. Finally, being small motors, they can operate in suitable conditions (low voltage required to operate the motor for example) and are much lighter.
The characteristics of the motor are as follows:

Table 11: Characteristics of the motor

	Model	**Weight**	**Power max**	**RPM max**	**Resistance**
Data	3080	1 650 kg	30 kW	52 500 rpm	3mΩ

Considering a nominal voltage of 60 V and a current of 247 A, we find that this motor reaches the nominal rotation number of the pump with an output power of 14.820 kW, and this corresponds to the power required for the proper functioning of the pump.
We carried out an initial thermal study of the motor in order to establish and determine the characteristics of the necessary cooling system. The main source of heating of an electric motor is due to the Joule effect. With our operating values (60V and 247A) and the considered motor (internal resistance of 3mΩ) we obtain $E = 183.027\,J$ dissipated every second. This amounts to a loss of 183.027 W. This heating power is therefore not negligible. It is imperative to reduce it as much as possible.
The cooling system must therefore be able to evacuate this heat as best as possible. Part of the cooling will be done naturally by convection. And most of the cooling will be done via a water-cooling shell. The shell is offered by the same company and will allow water to circulate around the engine to cool it.

To make this engine work we need a battery. The battery we are looking for must be capable of supporting the needs of the motor so that it can operate as desired. We have previously established that the motor would operate at a current of about 247 A and under 60 V. Knowing this we can determine that the battery must also operate at 60 V. We also need to know the capacity of the battery.
We must keep in mind the constraints of weight and space; the battery must be the least heavy and the least cumbersome possible. It may also be possible not to consider a single battery, but several that would then be arranged in series.
The batteries that were selected come from the manufacturer Tattu. They are the models Tattu 22.8V 25C 6S 23000 mAh. These batteries will make it possible to have an operating time of 5 mins. We will have to put 3 in series, which will give a voltage of 68.4 V, which is sufficient for our use.
Moreover, we need a dimmer and for that we chose the VESC 100/250 from Trampa.

3.7 Assembly

The assembly of the pump must be done in such a way that each part can be disassembled in order to inspect each of them.
First, we asked ourselves the question of the assembly of the mobile parts of the pump. For that, we took into account the mechanical constraints present, the constraints of ease of assembly as well as the manufacturing constraints. We therefore chose to make two distinct parts of the rotating assembly. The first part will be composed of the shaft and the

DOI: 10.13009/EUCASS2022-7674

impeller with keys so that the other part, the inducer, is an integral part of the assembly. This link will be maintained with an M4 screw, at the top of the impeller. The image below can illustrate it:

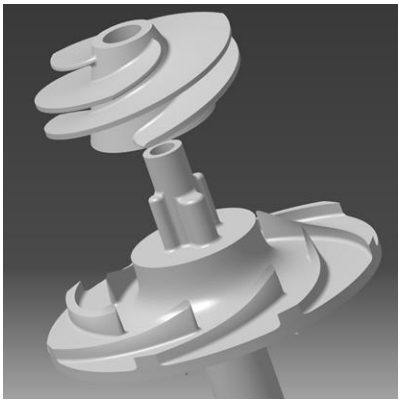

Figure 6: Assembly of the inducer and impeller

For the fixed part, the assembly will include more elements. The volute is in two parts, a first part which is the base of the volute and a second one the rest. This structure has been chosen to facilitate the sealing with the use of static O-rings. Then, the part containing the bearings and the dynamic seals will be decomposed in several parts in order to have access to these parts. The exact architecture is not completely defined since there are still some unknowns at the level of bearings and dynamic seals. We can see an exploded view of this assembly on the following figure:

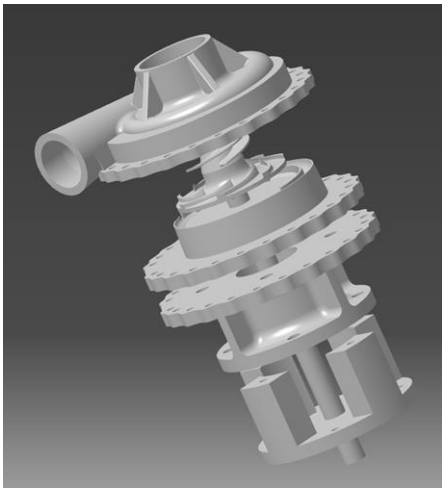

Figure 7: Assembly of the pump

There is one last assembly to be done. It is the connection between the motor and the pump shaft. For this we will use a coupling. In our case, the coupling must be able to resist the following constraints:

T Table 12: Constraints on the coupling

	RPM	**Torque**	**Shaft diameter**	**Features**
Data	45 450 rpm	3.8 N.m	8 mm	supports misalignment

We were able to find a coupling that meets these requirements. It comes from the distributor OLEK, and it is the model EKL-5-A-8-8 (size, elastomer type, inlet and outlet diameter).

3.8 Simulation

We have a motor pump that is theoretically complete, excluding bearings and seals, and that works. However, we need to do various simulations to validate our design. We decided to do static finite element simulations to check that the pump resists the pressure and the torque forces. Then, vibration simulations were done to make sure that the natural

DOI: 10.13009/EUCASS2022-7674

frequencies of the pump do not correspond to the rotation frequency. And finally, CFD simulation were ran to verify that the pump generates the right pressures.
For these simulations we used the software ANSYS and the Mechanical and Fluent solvers.
For the finite element simulations, we obtain the following results:

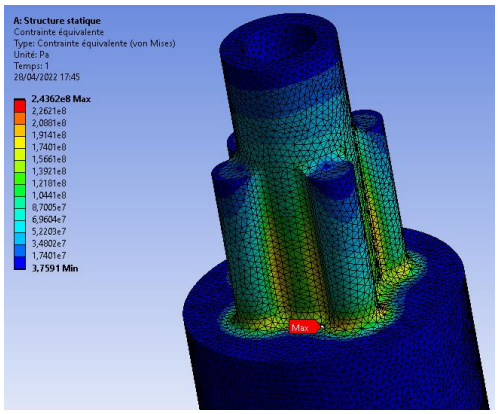

Figure 8: Stress simulation of the shaft

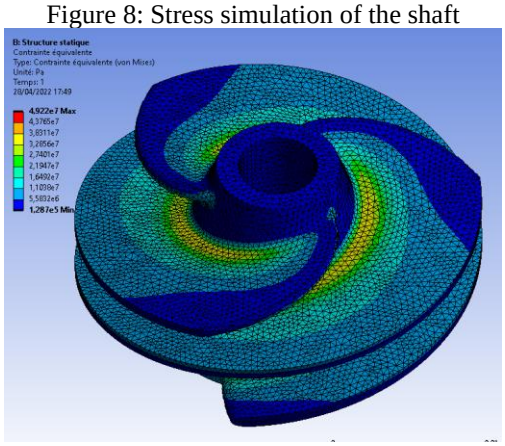

Figure 9: Stress simulation of the inducer

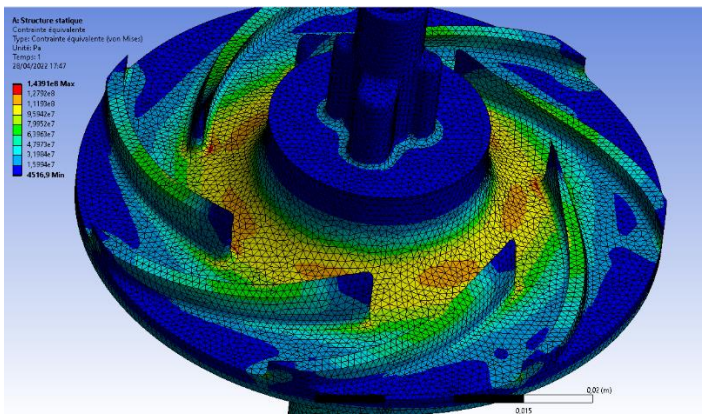

Figure 10: Stress simulation of the impeller

We can see that these simulations give us a maximum von Mises stress of $\sigma = 244\ MPa$. We therefore have a safety coefficient of 1.24 for water tests and greater than 2 with cryogenic temperatures. So, these simulations allow to confirm the resistance of the structure.

The vibratory simulations give us the following results:

DOI: 10.13009/EUCASS2022-7674

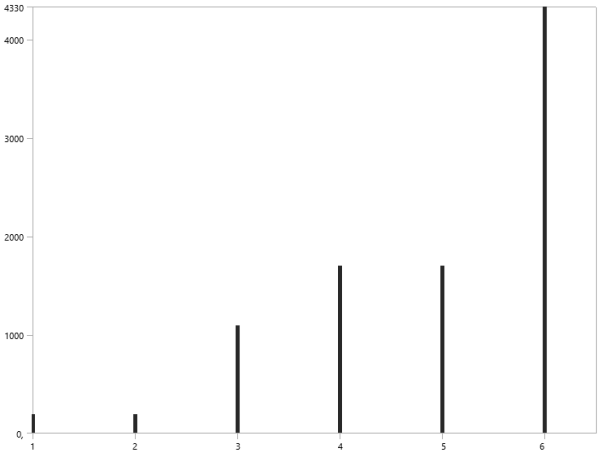

Figure 11: Vibratory simulation of the wheel

We can see the natural frequency and the corresponding rotation speed in the following table:

Table 13: Natural frequency of the pump

Mode	**1**	**2**	**3**	**4**	**5**	**6**
Frequency	185.24 Hz	185.28 Hz	1092.4 Hz	1694 Hz	1694.1 Hz	4330.4
RPM	11 114	11 117	65 520	101 640	101 646	259 824

Thanks to these simulations, we can see that we are far from the resonance frequencies with a rotation speed of 45 450 rpm. Therefore, there is no risk of having a resonance phenomenon of the impeller.

And finally, we made CFD simulations to validate our pump design. After initial simulations, we obtained with a flow of 2.45 kg/s, an output pressure of $P_2 = 43\ bar$ on average. However, we aim at a pressure of 52 bar. This difference is due to the slight modifications of the impeller made to facilitate its manufacture. By redoing some initial calculations, we could see that if we take 49 000 rpm, we could reach the 52 bar expected. After running the simulations again with this increase rotational speed, we obtain the following results:

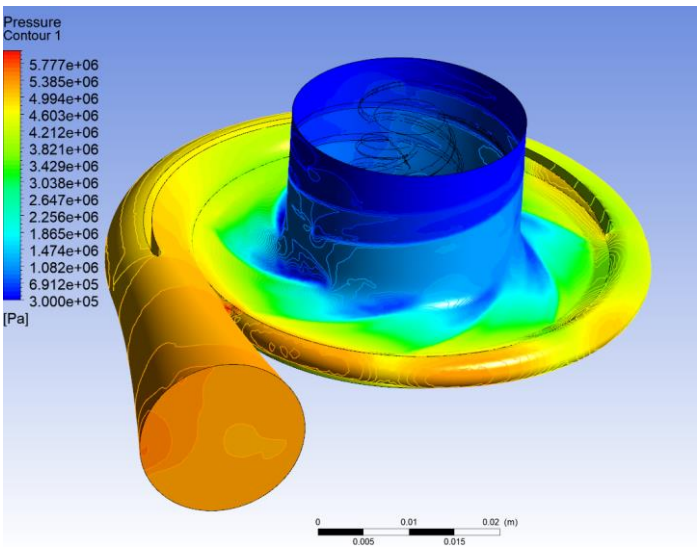

Figure 12: CFD simulation of the pump at 49 000 rpm

The results that this simulation gives us are that for an output flow of 2.461 kg/s for an average pressure $P_2 = 52.84$ bar. So, at a speed of 49 000 rpm, we find values corresponding to our specifications. Moreover, this speed can be reached with our motor and does not correspond to one of the natural frequencies of the wheel. And we can also notice that there is no big pressure drop (which implies a low risk of cavitation), as well as consistent speed profiles. We can therefore say that the pump is complete and meets the specifications

DOI: 10.13009/EUCASS2022-7674

4. Conclusion and perspective

This paper was able to present the different current advances on the oxygen motopump for a future version of the PERSEUS MINERVA engine. The design of the wheel is finished and validated by numerical simulations: CFD, finite element and vibratory. The design of the fixed part is largely finished, only the part containing the seals and the bearings will have to be finalized. No-load tests of the electric motor will be done soon. For the water tests of the pump, we will adapt the test bench, which the Innovative Propulsion Laboratory is building. And for tests with liquid oxygen, we will use the PERSEUS test bench in Vernon.
Thanks to motopumps, the MINERVA engine will be able to double its thrust. This is therefore quite an important development. Moreover, having pumps powered by an electric motor is less complex and more reliable than if they were powered by a turbine. However, the onboard weight will be higher due to the motors and batteries, which will limit the engine's performance but will allow a significant increase in thrust.

Acknowledgements

We would like to thank the CNES and the PERSEUS project for the trust they put in our team, as well as for their precious financial and technical support in addition to their valuable guidance in this project. We also thank IPSA, our university, for their logistical and financial support. Thanks to the support of all these partners, the Innovative Propulsion Laboratory keeps growing and improving its skills.

References

[1] P. Pempie. Turbopompes
[2] D. Huzel, D. Huang. Design of liquid propellant rocket engines. NASA. VI : 176-224